Archives of Materials Science and Engineering

Volume 96
Issue 2
April 2019
Pages 63-72

International Scientific Journal
published monthly by the
World Academy of Materials
and Manufacturing Engineering

DOI: 10.5604/01.3001.0013.2385

Influence of loads in the process of laying on the resource of sea pipelines

L. Poberezhny [a,*], S. Tregubenko [b], L. Poberezhna [c], A. Hrytsanchuk [d], A. Stanetsky [e]

[a] Department of Chemistry, Institute of Tourism and Geosciences, Ivano-Frankivsk National Technical University of Oil and Gas, 15, Karpatska str., Ivano-Frankivsk, Ukraine
[b] Central Research Institute of the Military Forces of Ukraine, 28b, Povitroflotskyy pr., Kyiv, Ukraine
[c] Department of Medical Informatics, Medical and Biological Physics, Pharmaceutical Faculty, Ivano-Frankivsk National Medical University, 12, Galytska str., Ivano-Frankivsk, Ukraine
[d] Department of Petroleum Production, Institute of Petroleum Engineering, Ivano-Frankivsk National Technical University of Oil and Gas, 15, Karpatska str., Ivano-Frankivsk, Ukraine
[e] Department of Military Training, Institute of Petroleum Engineering, Ivano-Frankivsk National Technical University of Oil and Gas, 15, Karpatska str., Ivano-Frankivsk, Ukraine
* Corresponding e-mail address: lubomyrpoberezhny@gmail.com

ABSTRACT

Purpose: In the process of laying on the bottom of the sea material of the pipeline undergoes single-cycle alternating load. The purpose of the work is to determine the effect of pre-operational loads on the resource of marine pipelines.

Design/methodology/approach: The influence of the method of construction of pipelines on their stress-strain state is analysed. According to the real modes of packing of sea pipelines, the loading regime is programmed and the laboratory modelling of the pipe-laying process by the S-method has been programmed.

Findings: According to the results of one-cycle shift load were obtained characteristics of the hysteresis loop. It is proposed to simplify the mathematical description of the hysteresis loop of the pipeline laying cycle in the given form. It was shown that the preload during the construction process negatively affects the durability of the pipeline material due to the exhaustion of its plasticity resource, reducing it to 70%.

Research limitations/implications: In the future, investigations into the effect of overloading and overloading during the repair of pipeline sections on their durability and on the safe exploitation of resources should be continued.

Practical implications: The developed method of estimation of influence of pre-operational loads in the process of pipeline laying on its safe exploitation resource is used in gas-extraction enterprises.

Originality/value: To forecast the deformation behaviour of the pipeline material in the laying cycle, it is efficient to use diagrams of a sign-changing single-cycle bend, which were built considering the creep. The fatigue life capability of a steel pipeline depends on the history of the pipeline load in the laying cycle. Ratio $\sigma^*_{0.2c} / \sigma^*_{0.2t}$ and $\varepsilon_{yc} / \varepsilon_{yt}$ can use as power and deformation criteria for evaluating Bauschinger effect. It is suggested that fatigue damage is determined by the width of the hysteresis loop.

Keywords: Subsea pipelines, Preoperational load, Corrosion fatigue, Kinetic of deformation, Resource of safe operation

Reference to this paper should be given in the following way:

L. Poberezhny, S. Tregubenko, L. Poberezhna, A. Hrytsanchuk, A. Stanetsky, Influence of loads in the process of laying on the resource of sea pipelines, Archives of Materials Science and Engineering 96/2 (2019) 63-72.

METHODOLOGY OF RESEARCH, ANALYSIS AND MODELLING

1. Introduction

When calculating sea pipelines, it is important to choose correctly the calculation scheme, which would allow using the existing level of development of calculation methods to determine the stress-deformed state due to loads and influences in different periods, and fully reflect the actual operating conditions of the pipeline. This approach allowed saving£ 5,000,000 in the process of the deep-water pipeline construction in the North Sea [1]. It should be noted that modern oil and gas pipelines in the North Sea are designed for a period of 30 years [1,2].

The calculation schemes and prospective methods of calculating the pipeline elements for strength are presented in detail in the works [3,4]. Therefore, we turn to the study of the practical possibility of problems solving considering nonlinearities [5,6].

It can be pointed out that in the future the elastic-plastic deformation will be considered as one of the reserves for more complete use of the bearing capacity of the sea pipeline [7,8]. In the calculations of pipelines constructions beyond the elasticity limit the diagrams of "stress – deformation" for pipe steel obtained experimentally are of supreme importance. It is also necessary to take into account the internal damage to the pipes [9,10]. For steel X-60 the diagram is shown in Figure 1a [11,12].

For practical calculations, the diagram $\sigma - \varepsilon$ is presented in the form of three sections (Fig. 1b): OA – elastic deformation; AB – elastic-plastic deformation; BC– strengthening (in the classical literature the sections AB and BC are associated with deformation strengthening of polycrystalline metal [13]). Only the section AB out of three sections is nonlinear. Four points of the diagram are considered as basic: the origin of the coordinates is the point O (0; 0); the limit of proportionality is the point A (σ_{pl}; ε_{pl}); the conditional deformation curve is the point B ($\sigma_{0,2}$; $\varepsilon_{0,2}$); strength limit is the point C (σ_b; ε_b). The limit of proportionality σ_{pl} is taken as $0.7\sigma_{0.2}$. Therefore, $\varepsilon_{pl} = \frac{0.7 \cdot \sigma_{0.2}}{E}$ According to the analysis and comparison of deformations obtained during tests on the destruction of samples by stretching and pipes by internal pressure, the deformation ε_b is taken as one-fifth of the relative elongation at break δ_5, that is, without taking into account the concentrated deformation in the neck ($\varepsilon_b = 0.2\ \delta_5$) [14,15].

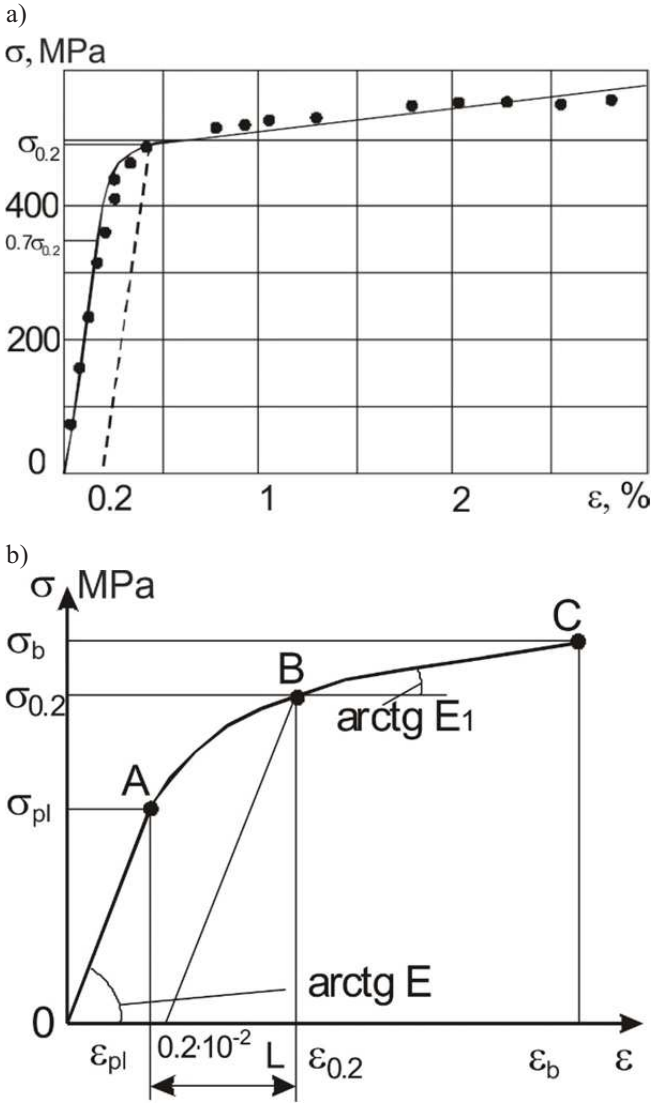

Fig. 1. Use of "stress-deformation" diagrams for pipelines calculation [11,12]

The linear sections of the diagram σ – ε are described by the following dependencies:

in the section OA ($0 \le \varepsilon \le \varepsilon_{pl}$)

$\sigma = E\varepsilon$,

in the section BC ($\varepsilon_{0.2} \le \varepsilon \le \varepsilon_b$)

$\sigma = \sigma_{0.2} + E_1(\varepsilon - \varepsilon_{0.2})$,

where

$$E_1 = \frac{\sigma_b - \sigma_{0,2}}{\varepsilon_b - \varepsilon_{0,2}} \cdot \varepsilon_{0,2} = \frac{\sigma_{0,2}}{E} + 0,2 \cdot 10^{-2}$$

The nonlinear section of the diagram (AB) is approximated by a function that meets the following conditions: to be monotone increasing, such that it is at least twice differentiated by the section [ε_{pl}; $\varepsilon_{0.2}$] and it is convex. The following condition meets such requirements:

$$\frac{d\sigma}{d\varepsilon} > 0; \quad \frac{d^2\sigma}{d\varepsilon^2} < 0; \quad \text{at } \varepsilon_{pl} \le \varepsilon \le \varepsilon_{0.2}.$$

For practical use the nonlinear part of the diagram σ – ε is proposed to be described by the equation

$$\sigma = \sigma_b + a \cdot \left(\varepsilon - \varepsilon_{pl}\right) + b \cdot \left[1 - \left(\frac{\varepsilon - \varepsilon_{pl}}{L}\right)^m\right],$$

where $a = 0,3\ \sigma_{0,2}/L$; $b = E - a$; $m_1 = (a - E_1)/b$.

Thus, the presence of a nonlinear section AB complicates the calculation of pipelines in general, taking into account elastic-plastic deformation. The presented diagrams (fig. 1) do not reflect the creep of metal and do not allow predicting its deformation behaviour at the repeated load with the opposite sign and is therefore ineffective for the study of changes in physical and mechanical properties of the material of sea pipelines during the laying and continuous operation. The miscellaneous stress-deformed state (SDS) characteristic to the main load-bearing elements of the linear part of the pipeline is not present at the specified scheme of load in experimental samples.

There appears a need for strain-kinetic analysis of the pipeline laying process using the S-method with the use of experimental studies of the transition from static to quasi-static load during the sign-changing cycle and from quasi-static to low-frequency load which appears after the pipeline is laid; as well as the development of diagrams of sign-changing single-cycle bending with advanced research capabilities for use in the sea pipelines designing.

When laying a sea pipeline by immersion, or by using a hinged curvilinear stinger, the section of the pipeline between the stern of the barge-pipe layer and the sea bottom gains the form of the S-shaped curve (Fig. 1). The stress on the curved section AB is regulated by the means of the tensioning device, and on a convex section BC it is limited by a stinger [16]. To improve the reliability of the pipe layer measuring equipment is used that allows controlling of the deflection line, strain and tension on the pipeline section from the barge stern to the seabed.

2. Experimental/theoretical details

With the increase of the laying depth and the pipeline diameter, as well as in case of strong cross-flow and rough sea, the complexity of engineering tasks increases significantly, in particular, in the part of the correct consideration in the calculation schemes of the conditions and technology of laying and in determining SDS. However, it does not sufficiently reflect the evolution of the S-shaped section (Fig. 2) and the related changes in outlines of the curve of the bending moments M from the distributed load, that ultimately leads to inaccuracies in the calculations and in the process of determination of the dangerous section area of the pipeline through which the greatest stresses are transmitted. In the section area where M reaches its maximum, the loss of stability of the initial cylindrical shape of the pipeline shell is possible [19-24].

Different methods of static and dynamic calculation of pipe laying can be found in the literature [11-13,17,18].

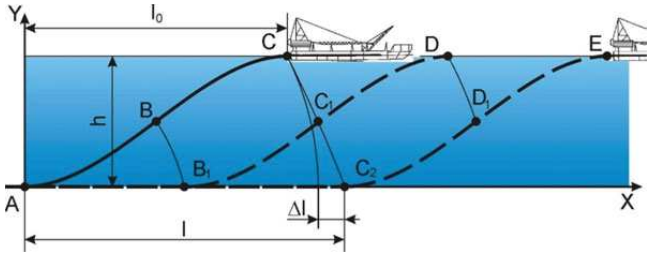

Fig. 2. The evolution of the S-shaped section of the pipeline

To simulate the work of the pipeline material (textured steel 20) in the section ABC (Fig. 1) and in the section of low cycle fatigue the cylindrical models-samples with l_p/d = 10 were used which were tested according to the developed method on the installation device MV-1K [25].

Let us consider (without taking into account the influence of waves and currents) the conditions for the transition of the ABC pipeline section to the horizontal position (Fig. 2). The projection of the section on the Y-axis represents the depth of the laying h, and its projection on the X-axis is expressed by the size l_0. Then the shortest distance between the points A and C is calculated as $l_s = \sqrt{h^2 + l_0^2}$. In its evolution process that was

studied in CorelDraw 17 according to the trajectories of characteristic points, the S-shaped section gets smooth and reaches the size l. Therefore, the increase of the section from the smoothing is $\Delta l = l - \sqrt{h^2 + l_0^2}$. The larger the increase of Δl, the more curved are the sections AB and BC and the greater is the probability of occurrence of plastic deformation in the dangerous pipe section area.

When moving a barge on the distance l there appears one load cycle, when the fibres of the pipe lying above the neutral layer, initially elongate (on the stinger), and then, with the approach to the bottom, shorten. Therefore, we propose to call the parameter l as the length of the laying in a load cycle.

To determine the period of the T_c cycle it is necessary to know the laying speed V_y and l. On the 70% of specialized and on all multipurpose pipe-laying vessels the method of pipeline extension on a horizontal montage platform with subsequent lowering under the tension on the stinger is used. This allows to lay a pipeline with a diameter of 1220 mm at a depth of h ≤ 300 m and with a diameter of up to 800 mm at a depth of h ≤ 700 m with V_y = 3-5 km/day [11]. The indicator l will depend on the length of the stinger, which can be 50-100 m [11], the diameter of the pipeline, the depth of laying, and the effort of tension. If we set l = 300 m, and V_y = 3 km/day, we get T_c = 2.4 h.

3. Results and discussion

In the study [26] the results of computer calculation of the deflections line and bending stresses σ during the pipeline laying by immersion at a depth of 45 mares presented. In the absence of the tension effort T the stress amplitude and curvature are the largest (Fig. 2), and the loading conditions for the pipe material are the most difficult. The main parameters of the stress cycle are the maximum stress σ_{max} = 400 MPa; minimum stress σ_{min} = -350 MPa; average stress σ_m = 25 MPa; amplitude of stress σ_a = 375 MPa; coefficient of asymmetry R_σ = -0.875.

For simulation on samples-models of the SDS change characteristic during the pipeline laying by immersion at T = 0, the shape to the cycle was set, as shown in Figure 4, curve *1*. This cycle differs from the previous (Fig. 3b) by the presence of step load and the absence of asymmetry of the stress cycle, which is done for the purpose of some complication of test conditions while maintaining the actual parameters *h, l, V_y and T_c*. With increasing or decreasing of the load at one degree, the nominal stress varied by a value Δσ = 20 MPa in load (unload) time $t_{l\ (u)}$ =1 sec. The endurance time at each degree t_e= 256.14 sec, and the total time $\Delta t = t_{l\ (u)} + t_e$ = 257.14 sec. The choice of the stress amplitude of σ_a = 420 MPa is based on the conclusions of work [26]. It was determined that the exploitation of the textured steel of the pipeline in the section of cyclic creep (above 420 MPa) is unacceptable, although the bearing capacity according to the bending moment in the static is far from exhausted.

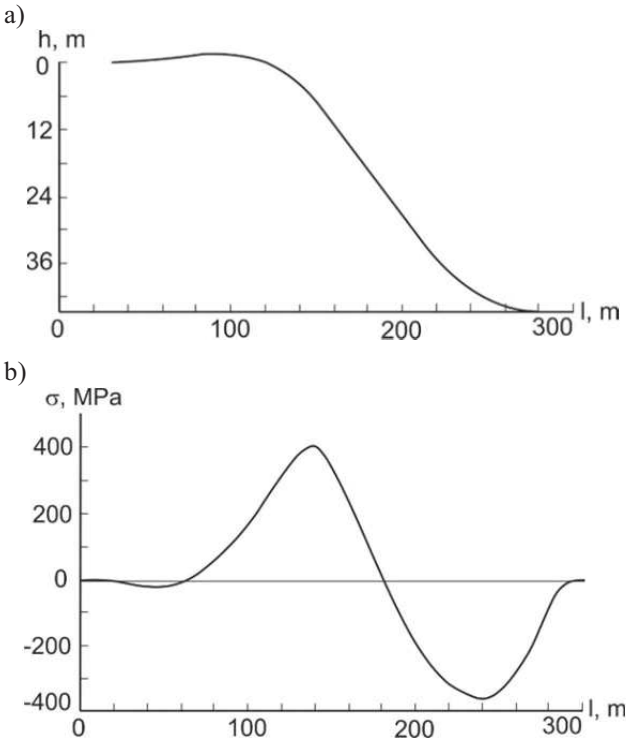

Fig. 3. Configuration of the bent axis (a) and stress distribution (b) in a pipeline with a diameter of 529 mm

The analysis of the deformation cycle shows (Fig. 4, curve 2) that in the conditions of a quasi-static load up to 420 MPa the low-temperature logarithmic creep over time t_e considerably appears at stresses greater than the yield limit $\sigma^*_{0,2}$ determined according to the developed method [27]. In the first half cycle the yield limit $\sigma^*_{0,2t}$ = 220 MPa, and in the second – $\sigma^*_{0,2c}$ = 165 MPa, and therefore we can present the bright display of the quasi-static Bauschinger effect and the related significant reduction of σ textured steel ($\sigma^*_{0,2c} / \sigma^*_{0,2t}$ = 0.75). The stress $\sigma^*_{0,2t}$ and $\sigma^*_{0,2c}$ correspond to the deformation ε_{yt} and ε_{yc} that are determined before the simulation of the complete hysteresis loop (Fig. 4). In order to find ε_{yc} it is necessary to find two

points on the curve 2, one of which corresponds to the stress, and the second $\sigma = 0$ at $T_c/2$. By the ratio $\varepsilon_{yc} / \varepsilon_{yt}$, we can further make conclusions about the effect of a single cycle load on the mechanical properties of the pipe steel. The ratio $\sigma^*_{0,2c} / \sigma^*_{0,2t}$ and $\varepsilon_{yc} / \varepsilon_{y\ t}$ is proposed to be considered as the force and deformation criteria for the Bauschinger effect estimation.

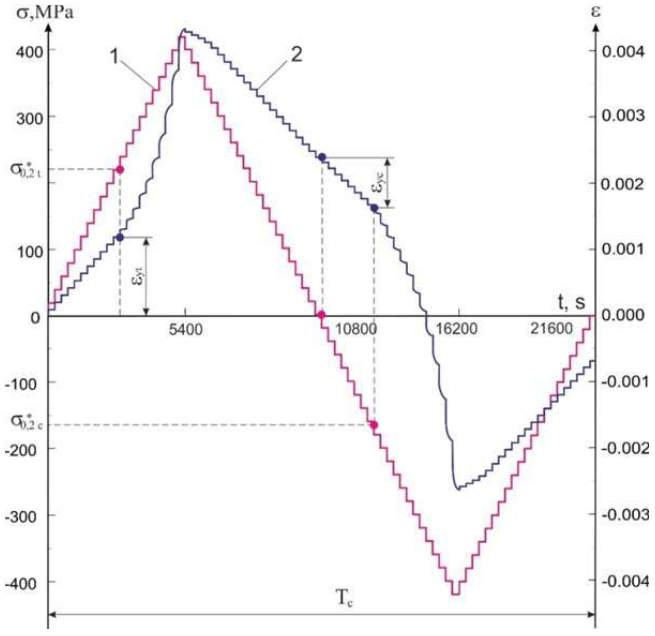

Fig. 4. Change in the stresses (1) and deformations (2) during the cycle period T_c

The deformation differences in loading and unloading, as well as the presence of the shift phases between σ and ε, ultimately lead to the formation of a mechanical hysteresis loop (Figs. 5, 6).

Such diagram, unlike the tension diagram, allows to forecast the deformation behaviour of the pipeline material in the laying cycle and to determine the parameters necessary for correct calculation of the SDS, namely: ε_{max}, ε_{min} – maximum and minimum deformations with the dimension of the stresses of the cycle $2\sigma_a$; ε_{yt}, ε_{yc} – deformations corresponding to the stress $\sigma^*_{0,2t}$ and $\sigma^*_{0,2c}$; ε_{pt}, ε_{pc} – width of the hysteresis loop in the first (odd) and the second (even) half cycle.

Since the diagram of the sign-changing single-cycle bend (hysteresis loop) is built according to the points corresponding to the value of ε after exposure at given σ, that is, by taking into account creep (Fig. 7), we can also determine the relaxed module of elasticity E_r and the conditional module of elasticity in the section of elastic-plastic deformation E_{pr}, as well as unrelaxed discharge module E_d.

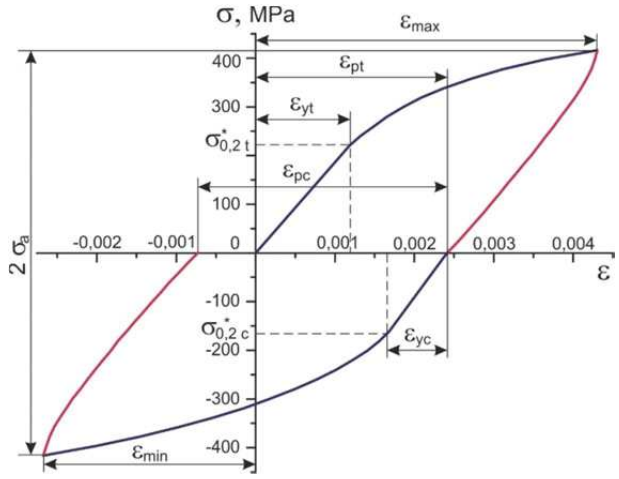

Fig. 5. Experimental hysteresis loop for textured steel 20 at the symmetrical cycle of bending stresses

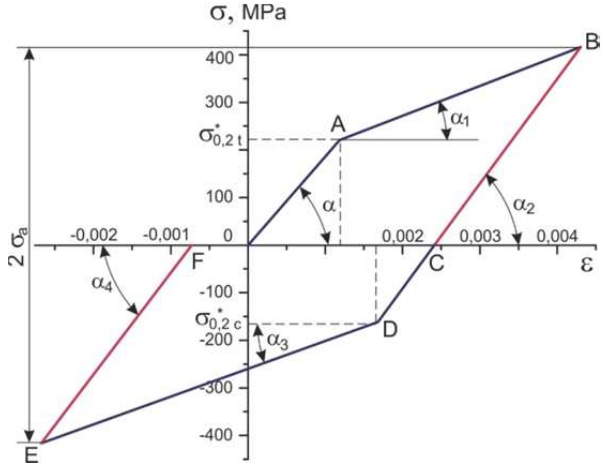

Fig. 6. Accepted hysteresis loop for textured steel 20 in the symmetrical cycle of bending stresses

The parameter E_{pr} will be more sensitive to the creep. As the process of low temperature creep of the pipe steel is of fading character, it is possible to draw an important practical conclusion that with the subsequent increase of t_e and, consequently, T_c, the dimension of the deformation will change slightly.

With a decrease of T_c, for example, up to 140 minutes, which is realized with the use of modern specialized and multi-purpose pipe laying vessels, t_e = 100 sec., and judging by the creep curves (Fig. 7), the neglecting of the value of ε_{cr} will mean extremely dangerous understatement of ε_{ma} and pipeline curvature.

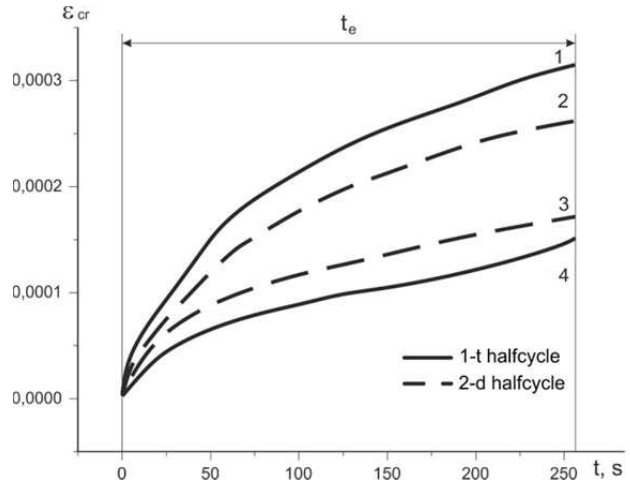

Fig. 7. Creep of textured steel 20: 1, 2 – 420 MPa; 3, 4 – 360 MPa

The characteristics of the pipe steel (absolute values) given in the Table 1 for the first and second half cycles show that the hysteresis loop we have adopted (Fig. 6), which consists of straight sloping sections can be used in the engineering calculations of the SDS.

Table 1.
Calculated characteristics of the textured steel 20 for the first and second half cycles

Number of half cycle. index	$\sigma^*_{0,2}$	E_r	E_{pr}	E_d	ε_{max}	ε_{min}	ε_y	ε_p
	MPa							
1 (t)	220	186424	62637	219716	0.00431	-	0.00118	0.00242
2 (c)	165	221576	58480	213898	-	0.00262	0.00074	0.00310

The values of tgα = E_{rt}, tgα$_1$ = E_{prt}, tgα$_2$ = E_{dt}, tgα$_3$ = E_{prc}, tgα$_4$ = E_{dc}, where E_{prt} and E_{prc} are relaxed conditional modules of elasticity in the sections of elastic-plastic deformation, and E_{dt} and E_{dc} are unrelaxed modules of discharge respectively for the first and second half cycles, as well as the coordinates of characteristic points are taken from the experimental hysteresis loop.

Then

$$\varepsilon_{\max} = \frac{\sigma^*_{0,2t}}{E_{rt}} + \frac{\sigma_a + \sigma^*_{0,2t}}{E_{prt}} \tag{1}$$

$$\varepsilon_{\max} = \frac{\sigma_a}{E_{dt}} + \varepsilon_{pt} \tag{2}$$

Solving equations (1) and (2) we can find the width of the hysteresis loop, which expresses residual deformation after discharge in the first half cycle:

$$\varepsilon_{pt} = \frac{1}{E_{prt}} \cdot \left[\sigma_a \cdot \left(1 - \frac{E_{prt}}{E_{dt}} \right) - \sigma^*_{0,2t} \cdot \left(1 - \frac{E_{prt}}{E_{rt}} \right) \right] \tag{3}$$

In the second half cycle the absolute values are

$$\varepsilon_{pc} = \frac{1}{E_{prc}} \cdot \left[\sigma_a \cdot \left(1 - \frac{E_{prc}}{E_{dc}} \right) - \sigma^*_{0,2c} \cdot \left(1 - \frac{E_{prc}}{E_{dt}} \right) \right] \tag{4}$$

$$\varepsilon_{\min} = \left(\varepsilon_{pc} - \varepsilon_{pt} \right) + \frac{\sigma_a}{E_{dc}} \tag{5}$$

With decreasing of σ_a and T_c, the angles α, α_2, $\alpha_4$and α_1, $\alpha_3$are getting closer. Therefore, for estimating calculations we can accept $E_{rt} \approx E_{rc} \approx E_{dt} \approx E_{dc}$ and $E_{prt} \approx E_{prc}$ and get simplified expressions:

$$\varepsilon_{pt} = \left(\sigma_a - \sigma^*_{0,2t} \right) \cdot \left(K_2 - K_1 \right) \tag{6}$$

$$\varepsilon_{pc} = \left(\sigma_a - \sigma^*_{0,2c} \right) \cdot \left(K_2 - K_1 \right) \tag{7}$$

where $K_1 = \frac{1}{E_{rt}}$ a $K_2 = \frac{1}{E_{prt}}$ – respectively, the coefficients of elastic and plastic deformation.

Using formulas (6) and (7) we can find the difference

$$\varepsilon_{pc} - \varepsilon_{pt} = \left(\sigma^*_{0,2t} - \sigma^*_{0,2c} \right) \cdot \left(K_2 - K_1 \right) \tag{8}$$

that is a value of one order with value $\varepsilon_{\max}$ (Fig. 5) and indicates intense cyclic softening of the textured steel 20 under experimental conditions and asymmetry of the deformation cycle ($R_\varepsilon \approx$ -0.608).

If you test pipes that were made using different technologies and from materials that have significantly different characteristics determined from the diagrams of a sign-changing single-cycle bend, there appears a practical need for a comparative evaluation according to the relative expansion (narrowing) of the hysteresis loop

$$\delta_h = \frac{\varepsilon_{pc} - \varepsilon_{pt}}{\varepsilon_{pt}} \approx \frac{1 - K_s}{\left(\frac{\sigma_a}{\sigma^*_{0,2t}} - 1 \right)} \tag{9}$$

where $K_s = \frac{\sigma^*_{0,2c}}{\sigma^*_{0,2t}}$ – power criterion for evaluating the Bauschinger effect.

The results of calculations by formulas (1)-(9) correlate well with the experimental data. For example, value $\delta_h = 0.2810$ which was determined directly from the experimental hysteresis loop. Substituting the corresponding stress values into formula (9), we get $\delta_h = 0.2806$.

Graphical analysis of the formula (8) shows (Fig. 4) that Bauschinger effect cannot be traced under $\sigma_{a_0} = \sigma^*_{0,2t}$ and $\varepsilon_{pc} - \varepsilon_{pt} = 0$ while during the dimension of the cycle stresses $2 \cdot \sigma_{a_1}$, the value K_s becomes minimal. That is, under $\sigma_{a_0} \le \sigma_a \le \sigma_{a_1}$ we get:

$$\frac{\sigma^*_{0,2c_1}}{\sigma^*_{0,2t}} \le K_s \le 1$$

Relative reduction of the yield limit in the half cycle of compression

$$K_s^{`} = \frac{\Delta\sigma^*_{0,2c}}{\sigma^*_{0,2c}}$$

where $\Delta\sigma^*_{0,2c} = \sigma^*_{0,2c} - \sigma^*_{0,2c_1}$

Relatively $K_s^{`} + K_s = 1$

When correctly determining the maximum allowable curvature of the pipeline in the laying cycle, it is necessary to take into account Bauschingerde formation $\Delta\varepsilon_b$, which will be significant for the textured steel 20 (Figs. 6-8).

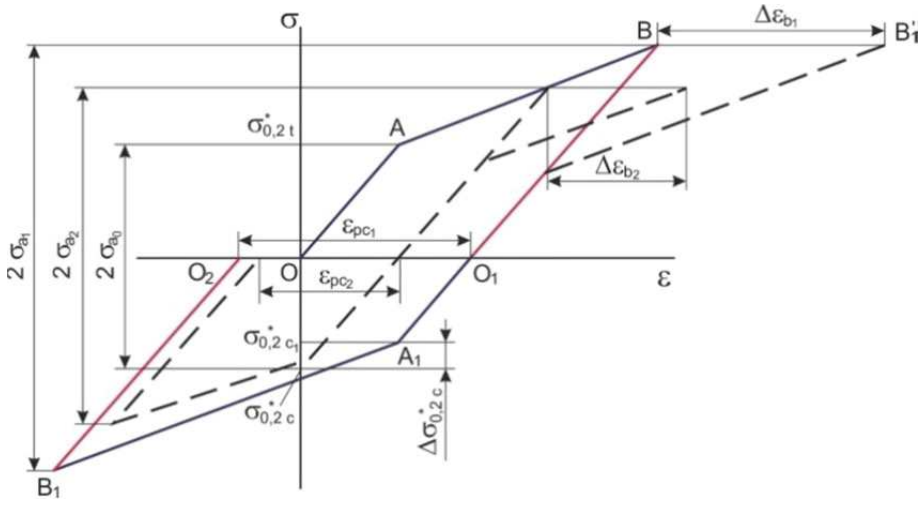

Fig. 8. Determination of quantitative characteristics of Bauschinger effect

Previously, it was determined [17] that at $\sigma > \sigma^*_{0,2t}$ the yield limit of the steel pipeline during the re-bending without changing the sign $\sigma^*_{0,2}$ is approximately equal to the maximum stress achieved at the first bend. Then, according to the construction (Fig. 4), $\Delta\varepsilon_{b_1} > \varepsilon_{pc_1}$, and $\Delta\varepsilon_{b_2} > \varepsilon_{pc_2}$ Thus, under such a graphical interpretation Bauschingerde formation is nothing more than the width of the hysteresis loop in the second half cycle [17].

After laying the pipeline the metal under the insulating coating during the exploitation will be exposed to low-frequency fatigue, which, depending on the amplitude of the stresses or deformations, can be small cyclic and multi-cyclic [28]. To detect the effect of the previous quasi-static load with the sign-changing cycle (Fig. 3) experimental studies were carried out on the fatigue life capability of the textured steel 20 at a frequency of 0.8 Hz in the air environment (Figs. 9, 10). It was determined that in the field of low cycle fatigue (σ_a = 370 MPa) the ratio is $N_0 / N_1 \approx 2$ where, respectively, N_0 and N_1 is the durability of previously undeformed and deformed sample-models.

Typical for both cases is a five-stage kinetics of deformation with characteristic peaks (Fig. 9) due to the successive passage of intensive, fleeting processes of cyclic softening (stage 1) and strengthening (stage 2). At stage 3 there appears a repeat softening of the textured steel, which has a fading character. The longest stage 4 corresponds to the stabilization of the amplitude of deformation ε_a. At the final stage 5 ε_a begins to increase with increasing intensity until the beginning of the final destruction [29]. It was determined that during the stabilization stage the fatigue process of previously deformed samples (Fig. 10)

compared with the previously undeformed ones, occurs at a slightly lower value ε_a, while $N_1 \approx 0.5 \cdot N_0$. This can be explained, on the one hand, by the different starting deformation amplitude.

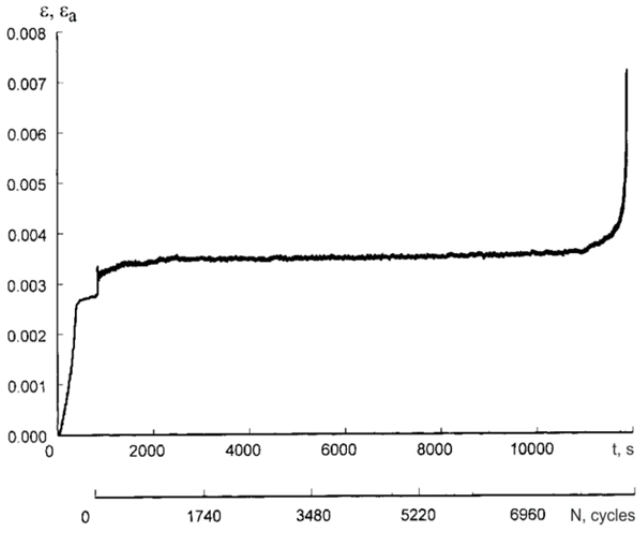

Fig. 9. Kinetic curve of deformation of previously undeformed textured steel 20 (370 MPa)

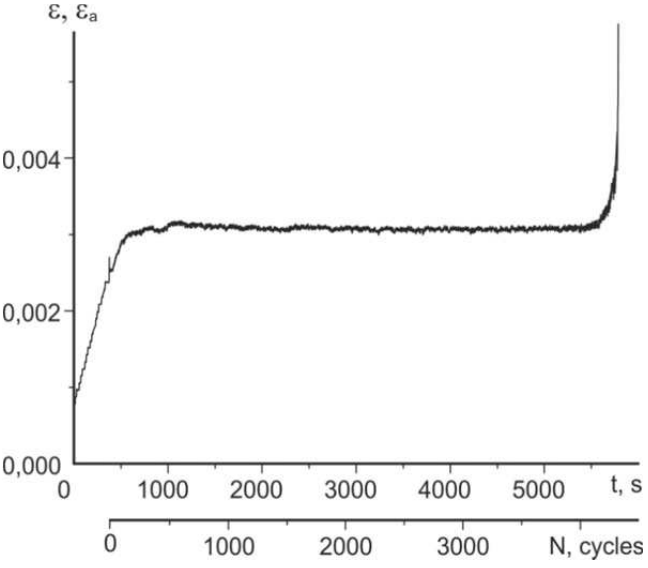

Fig. 10. Kinetic deformation curve of previously deformed textured steel 20 (370 MPa)

In previously undeformed samples it is smaller, since after a one-cycle load there appear residual deformations and, consequently, residual stresses, which lead to a linear dependence between σ and ε during the repeat static load without changing the sign (Fig. 6). On the other hand, an accumulation of damage appears in the conditions of previous quasi-static load, the negative effect of which on the durability is confirmed by the experiment.

It is suggested that fatigue damage is determined by the width of the hysteresis loop [30].

4. Conclusions

1. In the process of S-shaped section evolution there appears a one-cycle sign-changing quasi-static load on the pipeline element. To simulate the change of the SDS of marine pipeline element in the process of laying it is economically expedient to use cylindrical samples-models with $l_p/d = 10$, where the change in stress and deformation in time is monitored by the step load method at $R_\sigma = -1$ and the preservation of the real parameters h, l, V_y and T_c.
2. To forecast the deformation behaviour of the pipeline material in the laying cycle, it is efficient to use diagrams of a sign-changing single-cycle bend, which were built considering the creep.
3. Ratio $\sigma^*_{0,2c} / \sigma^*_{0,2t}$ and $\varepsilon_{yc} / \varepsilon_{yt}$ can use as power and deformation criteria for evaluating Bauschinger effect, and formulas (1)-(9) can be used rationally for analytical studies in the elastic-plastic deformation section.
4. The fatigue life capability of a steel pipeline depends on the history of the pipeline load in the laying cycle, which is experimentally confirmed by the kinetic deformation curves.

References

[1] S.D. De Groot, Quantitative assessment of the development of the offshore oil and gas industry in the North Sea, ICES Journal of Marine Science 53/6 (1996) 1045-1050.
[2] L. Bjerrum, Geotechnical problems involved in foundations of structures in the North Sea, Geotechnique 23/3 (1973) 319-358.
[3] S. Kyriakides, E. Corona, Mechanics of offshore pipelines: volume 1 buckling and collapse, Elsevier, 2007.
[4] S. Chandrasekaran, Dynamic analysis and design of offshore structures, New Delhi, Springer India, 2015.

[5] I. Adamiec-Wójcik, L. Brzozowska, Ł. Drąg, An analysis of dynamics of risers during vessel motion by means of the rigid finite element method, Ocean Engineering 106 (2015) 102-114.
[6] A. Torum, N.M. Anand, Free Span Vibrations of Submarine Pipelines in Steady Flows – Effect of Free-Stream Turbulence on Mean Drag Coefficients, Journal of Energy Resources Technology 107/4 (1985) 415-420.
[7] K.A. Anjinsen, Review of free spanning pipelines, Proceedings of the 5U' International Offshore and Polar Engineering Conference, Vol. 2: Golden (Colo), The Hague, 1995, 129-133.
[8] J.H. Prevost, Localization of deformations in elastic-plastic solids, International Journal for Numerical and Analytical Methods in Geomechanics 8/2 (1984) 187-196.
[9] L. Poberezhny, P. Maruschak, A. Hrytsanchuk, L. Poberezhna, O. Prentkovskis, A. Stanetsky, Impact of gas hydrates and long-term operation on fatigue characteristics of pipeline steels, Procedia Engineering 187 (2017) 356-362.
[10] A.V. Yavorskyi, M.O. Karpash, L.Y. Zhovtulia, L.Y. Poberezhny, P.O. Maruschak, Safe operation of engineering structures in the oil and gas industry, Journal of Natural Gas Science and Engineering 46 (2017) 289-295.
[11] YU.A. Horyayinov, Morski truboprovody, YU.A. Horyaynov, A.S. Fedorov, H.H. Vasylyevi (Eds.), M.: Nedra, 2001, 131 (in Russian).
[12] R.A. Aliev, Truboprovodnyj transport nefti i gaza, Ripol Klassik, 2013, 364 (in Russian).
[13] N. Hansen, Boundary strengthening in undeformed and deformed polycrystals, Materials Science and Engineering A 409/1-2 (2005) 39-45.
[14] YE.I. Kryzhanivskyy, Deformatsiyni efekty pry ukladenni truboprovodu na dno morya S-metodom, YE. I. Kryzhanivskyy, L. YA. Poberezhnyi, Naftova i hazova promyslovist 2 (2004) 35-39 (in Ukrainian).
[15] L. Poberezhnyi, P. Maruschak, O. Prentkovskis, I. Danyliuk, T. Pyrig, J. Brezinová, Fatigue and failure of steel of offshore gas pipeline after the laying operation, Archives of Civil and Mechanical Engineering 16/3 (2016) 524-536.
[16] E. Torselletti, L. Vitali, E. Levold, K.J. Mørk, Submarine Pipeline Installation JIP: Strength and deformation capacity of pipes passing over the S-lay vessel Stinger, Proceedings of the 25th International Conference on Offshore Mechanics and Arctic Engineering, Hamburg, 2006, 227-235.
[17] L.YA. Poberezhnyi, Urakhuvannya efektu Baushinhera pry proektuvanni morskykh truboprovodiv, Rozvidka ta rozrobka naftovykh i hazovykh rodovyshch 4/9 (2003) 48-54 (in Ukrainian).
[18] Z. Meng, X. Li, M. Yang, Z. Wang, S. Yang, H. Zhang, Dynamic load analysis of underwater pipeline, Proceedings of the International Symposium on Structural and Technical Pipeline Engineering, Beijing, 1992, 201-208.
[19] C.E. Murphey, C.G. Langner, Ultimate Pipe Strength Under Bending, Collapse, and Fatigue, Proceedings of the Offshore Mechanics and Arctic Engineering Conference, 1985.
[20] R.T. Igtand, T. Moan, Reliability analysis of deep water pipelines during laying, for combined pressure, tension and bending loads, Proceedings of the 3rd International Offshore and Polar Engineering Conference, Vol. 4: Golden(Colo), Singapore, 1993, 613-621.
[21] T.G. Johns, D.P. McConnell, Pipeline design resist buckling in deep water, Oil and Gas Journal 82/30 (1984) 62-65.
[22] T.Y. Corbishley, Pipeline free spans – design and operational consideration, International Society of Underwater Technology 9/1 (1983) 14-19.
[23] H. Cui, J. Tani, Effect of boundary condition on the stability of a pipe conveying fluid, Transactions of the JSME 60/570 (1994) 462-466.
[24] V.S. Tikhonov, A.I. Safronov, Dinamika svobodno visyashchego proleta podvodnogo truboprovoda, Tezisy dokladov nauch.-tekhn. konf. Problemmy morekhodnykh kachestv sudov i korabel'noy gidromekhaniki (38 Krylov-skiye chteniya, 1997), Sankt-Peterburg, 1997, 150-151 (in Russian).
[25] YE.I. Kryzhanivskyy, L.YA. Poberezhniy, Ustanovka dlya kompleksnykh doslídzhen malotsiklovoï vtomi materíalu morskikh truboprovodív u robochikh seredovishchakh, Naft. í gazova prom-st. 5 (2001) 44-45 (in Ukrainian).
[26] K.YA. Kapustin, M.A. Kamyshev, Stroitelstvo morskikh truboprovodov, M.: Nedra, 1982, 207 (in Ukrainian).
[27] YE.Í. Kryzhanivskyy, L.YA. Poberezhnyi, Deformatsíyna povedínka stalí truvodu pri nizkomkochastotíy vtomí, Zbirn. nauk. prats' IV Mízhnarodnogo simpoziumu "ISTF-2002", Ternopil': TDTU ím. Í. Pulyuya, Vol. 1, 2002, 296-300 (in Ukrainian).
[28] D.A. Kazakov, Modelirovaniye protsessov deformirovaniya i razrusheniya materialov i konstruktsiy, N.-Novgorod, D.A. Kazakov, S.A. Kapustin, YU. Korotkikh: Izd-vo Nizhegor. un-ta, 1999, 224 (in Russian).

[29] L.Y. Pobereznyi, L.Y. Poberezhna, P.O. Maruschak, S.V. Panin, Assessment of Potential Environmental Risks from Saline Soils Subsidence, in: IOP Conference Series: Earth and Environmental Science 50/1 (2017) 012046.

[30] V.T. Troshchenko, Mekhanicheskoye povedeniye materialov pri razlichnykh vidakh nagruzheniya, V.T. Troshchenko, A.A. Lebedev, V.A. Strizhalo, G.V. Stepnov, V.V. Krivenyuk, K.: Logos, 2000, 571 (in Russian).